PNWD-3015
BNFL-RPT-019 Rev. 0

Corrosion Tests of 316L and Hastelloy® C-22 in Simulated Tank Waste Solutions

Mike Danielson
Stan Pitman

February 2000

Prepared for BNFL, Inc. under
Project 29953
Battelle, Richland, Washington, 99352

LEGAL NOTICE

This report was prepared by Battelle Memorial Institute (Battelle) as an account of sponsored research activities. Neither Client nor Battelle nor any person acting on behalf of either:

MAKES ANY WARRANTY OR REPRESENTATION, EXPRESS OR IMPLIED, with respect to the accuracy, completeness, or usefulness of the information contained in this report, or that the use of any information, apparatus, process, or composition disclosed in this report may not infringe privately owned rights; or

Assumes any liabilities with respect to the use of, or for damages resulting from the use of, any information, apparatus, process, or composition disclosed in this report.

References herein to any specific commercial product, process, or service by trade name, trademark, manufacturer, or otherwise, does not necessarily constitute or imply its endorsement, recommendation, or favoring by Battelle. The views and opinions of authors expressed herein do not necessarily state or reflect those of Battelle.

CONTENTS

TABLES

Summary

Both the 316L stainless steel and Hastelloy® C-22 gave satisfactory corrosion performance in the simulated test environments. They were subjected to 100 day weight loss corrosion tests and electrochemical potentiodynamic evaluation.

1.0 Introduction

This activity supports confirmation of the design basis for the materials of construction of process vessels and equipment used to handle the feed to the LAW-melter evaporator. BNFL process and mechanical engineering will use the information derived from this task to select material of construction for process vessels and equipment. The two materials under investigation are 316L stainless steel and Hastelloy® C-22.

2.0 Experimental Test Conditions

2.1 Immersion Corrosion Tests

Immersion tests were carried out using the methods reported in ASTM procedure ASTM-G-31-72, *Standard Practice for Laboratory Immersion Corrosion Testing for Metals* (ASTM 1998). The two alloys under consideration are 316L and Hastelloy® C-22 (See Table 1 for composition.). Test specimens had dimensions of approximately 5.0 by 2.5 by 0.32 cm (2 by 1 by 1/8 inch) with a hole in one end (for mounting) giving a total area of approximately 30.6 cm^2. The dimensions of each specimen were measured and recorded. The specimens were cleaned by washing in soap solution, followed by a DI water rinse, and then a high purity ethanol rinse before being air dried and weighed to the nearest 0.1 mg.

Each test apparatus consisted of a 3,000-ml Teflon® container with a condenser in the center of the lid, a type-K thermocouple (sheathed in Inconel® 600), and a magnetic stirring bar. The entire container was placed in a glass-lined resin kettle heater which was placed over a magnetic stirring apparatus for continuous agitation. The temperature was controlled at the test temperatures using a separate temperature controller for each container. A corrosion rack was constructed from corrosion resistant titanium for each container. Test specimens were immersed in the test solution, suspended at the vapor-liquid interface, suspended in the vapor space above the test solution (no condensation), and suspended under the reflux condenser in the vapor space (condensation). The specimens were insulated from each other and the rack by using Teflon® tubing and Teflon® spacers. One liter of each of the three test solutions was added to each test container. The test solutions and temperature conditions are identified in Table 2. The original duration of the tests was to be 4 months, but was shortened to 100 days with concurrence from BNFL. The immersion tests started 3/22/99 and were terminated on 7-1-99 for about 100 days of immersion time. The boiling tests required periodic additions of DI water to maintain the liquid level, amounting to approximately 35ml every week. The liquid depth was determined using a wire as the depth gage and identifying contact with the solution meniscus by measuring the alternating current conductivity.

At the end of the testing period, the specimens were removed, washed in DI water and ethanol and then photographed. The specimens were then acid cleaned and evaluated in accordance with

ASTM-G-1-90 and ASTM-G-31-72, and the average uniform penetration rate was calculated by weight loss. The C-22 specimens were cleaned in 10% nitric acid (60°C) for 30 minutes to remove the scale. In a number of cases, the C-22 specimens weighed a few tenths of a milligram more than the starting weight because this gentle acid treatment did not completely remove the oxide which had thickened during the test exposure. Under these conditions, the weight loss (initial weight minus final weight) was assigned a zero value to calculate the penetration rate. The 10% nitric acid (60°C) for 30 minutes treatment was not adequate the remove the corrosion deposits on the 316L stainless steel. Therefore, the more aggressive CP-9 was employed (500 ml DI water + 500 ml concentrated HCl + 25 ml formaldehyde for 30 minutes at ambient temperature) (NACE 1976). Weight loss measurements were carried out on blanks (uncorroded specimens) to determine metal loss from exposure to the cleaning solution, but this compensation was only needed for the 316L specimens. Each specimen was visually examined for localized attack and a visual corrosion assessment was reported. The specimens were then photographed in the cleaned condition. The photographs are shown in Appendix 2. Results of the immersion tests are presented in Section 4.0.

2.2 Electrochemical Testing

After the immersion tests were completed, the simulant solutions were then used for the electrochemical polarization tests. These tests are based upon ASTM procedure ASTM-G-5-94, *Standard Reference Test Method for Making Potentiostatic and Potentiodynamic Anodic Polarization Measurements*. Each specimen was polished using 600 grit SiC paper, immersed in the test solution and the open-circuit potential recorded after 55 minutes immersion. Immediately, the cyclic polarization test was started. The polarization started at the open circuit potential and went to 0.8 volts anodic (relative to the open circuit potential) and then returned, going to a -.2 volts (relative to the open circuit potential), all at a rate of 0.167 mV/s. The BNFL test specification required that the tests be run in duplicate at temperatures of 25^{O}C, 50^{O}C, and approximately 100^{O}C (boiling) . The reference electrode was a saturated calomel electrode (SCE) at ambient temperature and connected to the test solution by a salt bridge. The specimen was a round disk mounted in a PAR (Princeton Applied Research, Princeton, NJ) electrode holder of 1 cm^2 surface area. The test solution was contained in a PAR glass 1-liter flask containing a Teflon® coated stir bar and was under a continuous nitrogen gas purge. The test solution was stirred using a external magnetic stirrer and heated using a heating mantle and temperature controller. The thermocouple (Inconel® 600 sheathed) entered the flask through the condenser. A Gamry potentiostat Model PC4/750 (Langhorne, PA) was used to control and record the current-potential data. At the end of each test, each specimen was visually examined for localized attack (pitting and crevice corrosion under the gasket).

The potentiodynamic technique is useful to determine if there is an electrochemical potential regime where the material is prone to pitting or crevice attack. This behavior is signified by a large hysteresis loop in the current-potential plot; that is, the current on the return scan is considerably larger than the initial current (at the same potential). The current-potential plots are shown in Appendix 3 as Figures 1-12. The results are discussed in Section 4.0.

3.0 Quality Control

This work was conducted in accordance with a BNFL approved quality assurance plan that implements the requirements of 10 CFR 830.120. An approved Test Plan (Test Plan 1999) was written before the testing started.

Table 1. Metal Composition (w%)

alloy	C	Mn	P	S	Si	Cr	Ni	Mo	Cu	Co	Other	Other
316L	.015	1.81	.026	.001	.27	16.30	10.15	2.11	.34	.28	.049 N	Bal Fe
C22	.002	.19	<.005	.008	.026	21.30	bal	13.08	-	1.82	4.00 Fe	2.93 W

Table 2. Test Solutions for Immersion Corrosion Test (non radioactive)

Organization	Solution	Temperature
Battelle	Simulated Envelope A Stream 75 Feed to LAW Melter Feed Evaporator (BNFL 1998a)	50^{O}C and Boiling point
Battelle	Simulated Envelope B Stream 75 Feed to LAW Melter Feed Evaporator (BNFL 1998b).	50^{O}C and Boiling point
Battelle	Simulated Envelope C Stream 75 Feed to LAW Melter Feed Evaporator (BNFL 1998c).	50^{O}C and Boiling point

4.0 Test Results

The immersion testing indicates no significant differences between the 316L stainless steel and Hastelloy® C-22. The 316L material showed some slight attack in simulant A at the vapor/liquid interface at the boiling point but depth of attack was shallow. Corrosion rates were slightly higher at the boiling point than at 50°C, but the differences were not important.

The electrochemical tests, due to their complexity, require some explanation. Electrochemical testing can indicate how close the material is to failing by localized corrosion processes. It is possible to create a relatively benign environment in a weight loss test environment such that the material behaves in an acceptable manner; yet, when in the real plant environment, the fluctuating chemistry conditions can create an environment where the material has an unacceptable behavior. The potentiodynamic test permits an evaluation of whether the material is really on the edge of acceptability. The data are shown in Appendix 3 for both scans (duplicate scans were carried out). The "start" and "stop" data refers to the first scan, and the arrows assist in showing the direction of the first scan (whether the potential is increasing or decreasing with time). The significant characteristic in the current-potential behavior that denotes localized attack (pitting and crevice corrosion) is the hysteresis loop which forms immediately upon reversal of the potential upon reaching the maximum anodic potential. The current increase is due to pitting and crevice corrosion that initiates and rapidly propagates but then becomes fairy independent of the potential. If the hysteresis loop does not form until several hundreds of millivolts have passed as the potential moves from the maximum potential back to the open circuit potential, this can be an indication of the

electrochemical reduction of the passive film that was grown during the anodic phase of the scan. A visual examination of the electrode is necessary after the scan to insure the correct interpretation.

Except for the cases noted below, the potentiodynamic behavior indicated no localized attack was present. For the 316L material, solution C and solution B did not lead to localized attack, based on a **visual** specimen examination following the potentiodynamic experiment. The 316L had a characteristic hysteresis loop that might denote localized attack in solution C at 50°C and the second scan at 103°C, but the visual examination after the test did not indicate any localized attack. The results in solution A were similar to B and C except that **one** test (repeat scan) at 104°C revealed numerous incipient pits that were identified by the visual examination—the current-potential scan did not clearly indicate localized attack was present. The pits were not deep enough to characterize their depth by optical means. The author has no explanation for the three false indications of localized attack. It was concluded that the behavior of 316L was adequate in all three test environments, replicating the results from the immersion testing.

The C22 material showed no indication of localized attack from the current-potential behavior in all three test environments. One of the visual examinations at the end of repeat test in solution B at 100°C indicated a small amount of crevice attack under the gasket (too shallow measure), but this behavior was not observed on the first test. Only the second scan is shown for the data in Figure A3-14 because during the first scan, the electrical leads to the working electrode and counter electrode were accidentally crossed. It was concluded that the behavior of C22 was adequate in all three test environments, replicating the results from the weight loss testing.

5.0 Conclusions

The weight loss results and visual observations indicate that there are no corrosion problems associated with the Hastelloy® C-22 in the environmental conditions studied in this test program. On two occasions, there were a few shallow pits observed but they were too shallow to measure (below 0.0005 inches or 0.01 mm depth). The electrochemical results support the weight loss results.

The 316L material also shows no corrosion problems except at the vapor/liquid region of simulant A under boiling conditions, and here the rate was a negligible 0.5 mpy (.01 mm/y). More importantly, there was no knifeline attack observed at this region. The electrochemical results support the weight loss results. The two alloys have a similar corrosion behavior, based on the results from the immersion tests and electrochemical tests.

6.0 References

ASM Handbook. 1990. "Volume 1, Properties and Selection: Irons, Steels, and High-Performance Alloys." Page 854. Materials Park, Ohio.

ASTM-G-1-90, *Standard Practice for Preparing, Cleaning, and Evaluating Corrosion Test Specimens*, 1998 Annual Book of ASTM Standards, volume 03.02 – Wear and Erosion; Metal Corrosion, American Society of Testing and Materials, Philadelphia, Pennsylvania.

ASTM-G-5-94, *Standard Reference Test Method for Making Potentiostatic and Potentiodynamic Anodic Polarization Measurements*, 1998 Annual Book of ASTM Standards, volume 03.02 – Wear and Erosion; Metal Corrosion, American Society of Testing and Materials, Philadelphia, Pennsylvania.

ASTM-G-31-72, *Standard Practice for Laboratory Immersion Corrosion Testing of Metals*, 1998 Annual Book of ASTM Standards, volume 03.02 – Wear and Erosion; Metal Corrosion, American Society of Testing and Materials, Philadelphia, Pennsylvania.

ASTM-G-75-95, Standard Test Method for Determination of Slurry Abrasivity (Miller Number) and Slurry Abrasion Response of Materials (SAR Number), 1998 Annual Book of ASTM Standards, volume 03.02 – Wear and Erosion; Metal Corrosion, American Society of Testing and Materials, Philadelphia, Pennsylvania.

BNFL 1998a, Flowsheet Mass Balance Report LAW/HLW Option – LAW Envelope A, October 2, 1998, BNFL Engineering Ltd., Salford Quays, Manchester U.K.

BNFL 1998b, Flowsheet Mass Balance Report LAW/HLW Option – LAW Envelope B, October 2, 1998, BNFL Engineering Ltd., Salford Quays, Manchester U.K.

BNFL 1998c, Flowsheet Mass Balance Report LAW/HLW Option – LAW Envelope C, October 2, 1998, BNFL Engineering Ltd., Salford Quays, Manchester U.K.

Miller, Jim. August 24, 1999. Phone (281-446-0041) call to White Rock Engineering, Humble, TX 77396.

NACE. 1976. TM-01-69, Laboratory Corrosion Testing of Metals for Process Industries. Nat. Assoc. Corrosion Engineers. Houston, TX.

Test Plan. 1999. "Materials Corrosion, Erosion, and Plate-out Test Specification." Document number BNFL-TP-29953-019. Written by MJ Danielson and SG Pitman, PNNL, Richland, WA.

WHC 1989, *Hanford Waste Vitrification Project Technical Manual*, revision 13, section 4.7 Equipment Construction Materials, Westinghouse Hanford Company, Richland, Washington.

WSRC 1996, *Materials Performance in a High-Level Radioactive Waste Vitrification System*, WSRC-MS-96-0356, revision 0, Westinghouse Savannah River Company, Aiken, South Carolina.

Appendix 1. Corrosion Data

Solution ID	Condition	Specimen ID#	Corr. Rate, mpy	Corr. Rate, mm/y	Observations
BP Sim A	liquid	316-067	0.076	0.0019	NA
BP Sim A	liquid	316-068	0.082	0.0021	NA
BP Sim A	vapor/liquid	316-069	0.526	0.0134	general attack in liquid phase, no knifeline attack
BP Sim A	vapor/liquid	316-070	0.504	0.0128	general attack in liquid phase, no knifeline attack
BP Sim A	vapor/condensate	316-071	0.115	0.0029	no localized attack
BP Sim A	vapor/condensate	316-072	0.068	0.0017	no localized attack
BP Sim A	vapor	316-073	0.034	0.0009	no localized attack
BP Sim A	vapor	316-074	0.039	0.0010	no localized attack
BP Sim A	liquid	C22-009	0.199	0.0051	NA
BP Sim A	liquid	C22-010	0.199	0.0050	NA
BP Sim A	vapor/liquid	C22-011	0.248	0.0063	NA
BP Sim A	vapor/liquid	C22-012	0.234	0.0059	NA
BP Sim A	vapor/condensate	C22-013	0.003	0.0001	NA
BP Sim A	vapor/condensate	C22-014	0.005	0.0001	NA
BP Sim A	vapor	C22-015	0.000	0.0000	NA
BP Sim A	vapor	C22-016	0.000	0.0000	NA
BP Sim B	liquid	316-041	0.000	0.0000	NA
BP Sim B	liquid	316-042	0.000	0.0000	NA
BP Sim B	vapor/liquid	316-043	0.025	0.0006	NA
BP Sim B	vapor/liquid	316-044	0.025	0.0006	NA
BP Sim B	vapor/condensate	316-045	0.010	0.0003	NA
BP Sim B	vapor/condensate	316-046	0.000	0.0000	NA
BP Sim B	vapor	316-047	0.000	0.0000	NA
BP Sim B	vapor	316-048	0.000	0.0000	NA
BP Sim B	liquid	C22-033	0.029	0.0007	NA
BP Sim B	liquid	C22-034	0.029	0.0007	2 shallow pits--too shallow to measure depth
BP Sim B	vapor/liquid	C22-035	0.013	0.0003	NA
BP Sim B	vapor/liquid	C22-036	0.011	0.0003	NA
BP Sim B	vapor/condensate	C22-037	0.000	0.0000	NA
BP Sim B	vapor/condensate	C22-038	0.000	0.0000	NA
BP Sim B	vapor	C22-039	0.000	0.0000	NA
BP Sim B	vapor	C22-040	0.000	0.0000	NA
BP Sim C	liquid	316-049	0.000	0.0000	NA
BP Sim C	liquid	316-050	0.000	0.0000	NA
BP Sim C	vapor/liquid	316-051	0.020	0.0005	NA
BP Sim C	vapor/liquid	316-052	0.024	0.0006	NA
BP Sim C	vapor/condensate	316-053	0.011	0.0003	NA
BP Sim C	vapor/condensate	316-054	0.009	0.0002	NA
BP Sim C	vapor	316-055	0.000	0.0000	NA
BP Sim C	vapor	316-056	0.000	0.0000	NA
BP Sim C	liquid	C22-041	0.004	0.0001	1 shallow pit--too shallow to measure depth
BP Sim C	liquid	C22-042	0.001	0.0000	NA
BP Sim C	vapor/liquid	C22-043	0.059	0.0015	NA
BP Sim C	vapor/liquid	C22-044	0.053	0.0014	NA
BP Sim C	vapor/condensate	C22-045	0.020	0.0005	NA
BP Sim C	vapor/condensate	C22-046	0.009	0.0002	NA
BP Sim C	vapor	C22-047	0.007	0.0002	NA
BP Sim C	vapor	C22-048	0.007	0.0002	NA
NA = no significant attack (includes no localized attack)					

Solution ID	Condition	Specimen ID#	Corr. Rate, mpy	Corr. Rate, mm/y	Observations
50C Sim A	liquid	316-075	0.000	0.0000	NA
50C Sim A	liquid	316-076	0.000	0.0000	NA
50C Sim A	vapor/liquid	316-077	0.010	0.0002	NA
50C Sim A	vapor/liquid	316-078	0.000	0.0000	NA
50C Sim A	vapor/condensate	316-079	0.005	0.0001	NA
50C Sim A	vapor/condensate	316-080	0.006	0.0002	NA
50C Sim A	vapor	316-081	0.000	0.0000	NA
50C Sim A	vapor	316-082	0.000	0.0000	NA
50C Sim A	liquid	C22-017	0.000	0.0000	NA
50C Sim A	liquid	C22-018	0.000	0.0000	NA
50C Sim A	vapor/liquid	C22-019	0.000	0.0000	NA
50C Sim A	vapor/liquid	C22-020	0.000	0.0000	NA
50C Sim A	vapor/condensate	C22-021	0.000	0.0000	NA
50C Sim A	vapor/condensate	C22-022	0.000	0.0000	NA
50C Sim A	vapor	C22-023	0.000	0.0000	NA
50C Sim A	vapor	C22-024	0.000	0.0000	NA
50C Sim B	liquid	316-059	0.000	0.0000	NA
50C Sim B	liquid	316-060	0.000	0.0000	NA
50C Sim B	vapor/liquid	316-061	0.000	0.0000	NA
50C Sim B	vapor/liquid	316-062	0.000	0.0000	NA
50C Sim B	vapor/condensate	316-063	0.000	0.0000	NA
50C Sim B	vapor/condensate	316-064	0.000	0.0000	NA
50C Sim B	vapor	316-065	0.000	0.0000	NA
50C Sim B	vapor	316-066	0.000	0.0000	NA
50C Sim B	liquid	C22-001	0.000	0.0000	NA
50C Sim B	liquid	C22-002	0.000	0.0000	NA
50C Sim B	vapor/liquid	C22-003	0.000	0.0000	NA
50C Sim B	vapor/liquid	C22-004	0.000	0.0000	NA
50C Sim B	vapor/condensate	C22-005	0.000	0.0000	NA
50C Sim B	vapor/condensate	C22-006	0.000	0.0000	NA
50C Sim B	vapor	C22-007	0.000	0.0000	NA
50C Sim B	vapor	C22-008	0.000	0.0000	NA
50C Sim C	liquid	316-083	0.000	0.0000	NA
50C Sim C	liquid	316-084	0.000	0.0000	NA
50C Sim C	vapor/liquid	316-085	0.000	0.0000	NA
50C Sim C	vapor/liquid	316-086	0.000	0.0000	NA
50C Sim C	vapor/condensate	316-087	0.000	0.0000	NA
50C Sim C	vapor/condensate	316-088	0.000	0.0000	NA
50C Sim C	vapor	316-089	0.000	0.0000	NA
50C Sim C	vapor	316-090	0.000	0.0000	NA
50C Sim C	liquid	C22-025	0.000	0.0000	NA
50C Sim C	liquid	C22-026	0.000	0.0000	NA
50C Sim C	vapor/liquid	C22-027	0.000	0.0000	NA
50C Sim C	vapor/liquid	C22-028	0.000	0.0000	NA
50C Sim C	vapor/condensate	C22-029	0.000	0.0000	NA
50C Sim C	vapor/condensate	C22-030	0.000	0.0000	NA
50C Sim C	vapor	C22-031	0.000	0.0000	NA
50C Sim C	vapor	C22-032	0.000	0.0000	NA
NA = no significant attack (includes no localized attack)					

Appendix 2. Cleaned Specimens

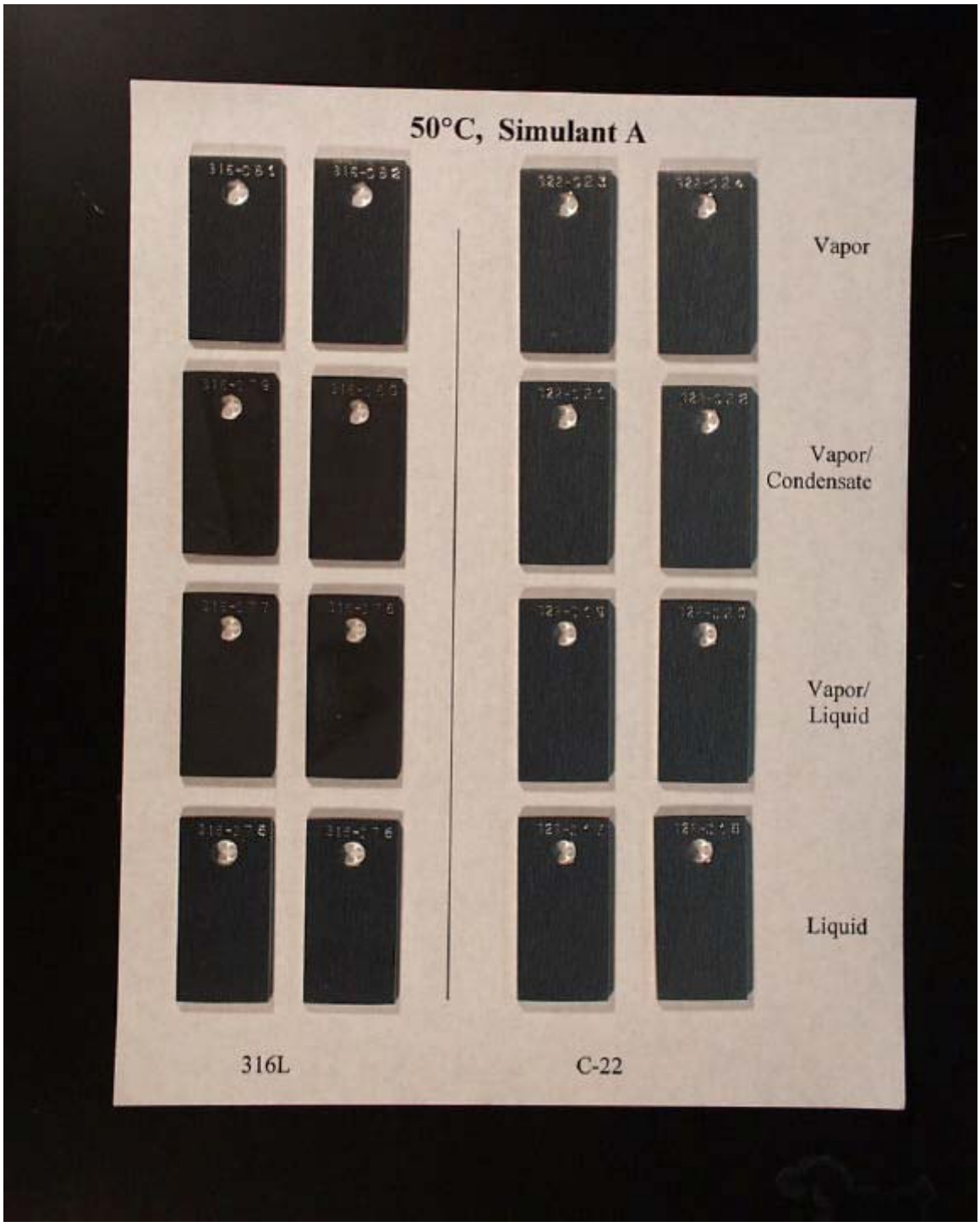

Figure A2-1. Specimens exposed to Simulant A at 50°C, after cleaning.

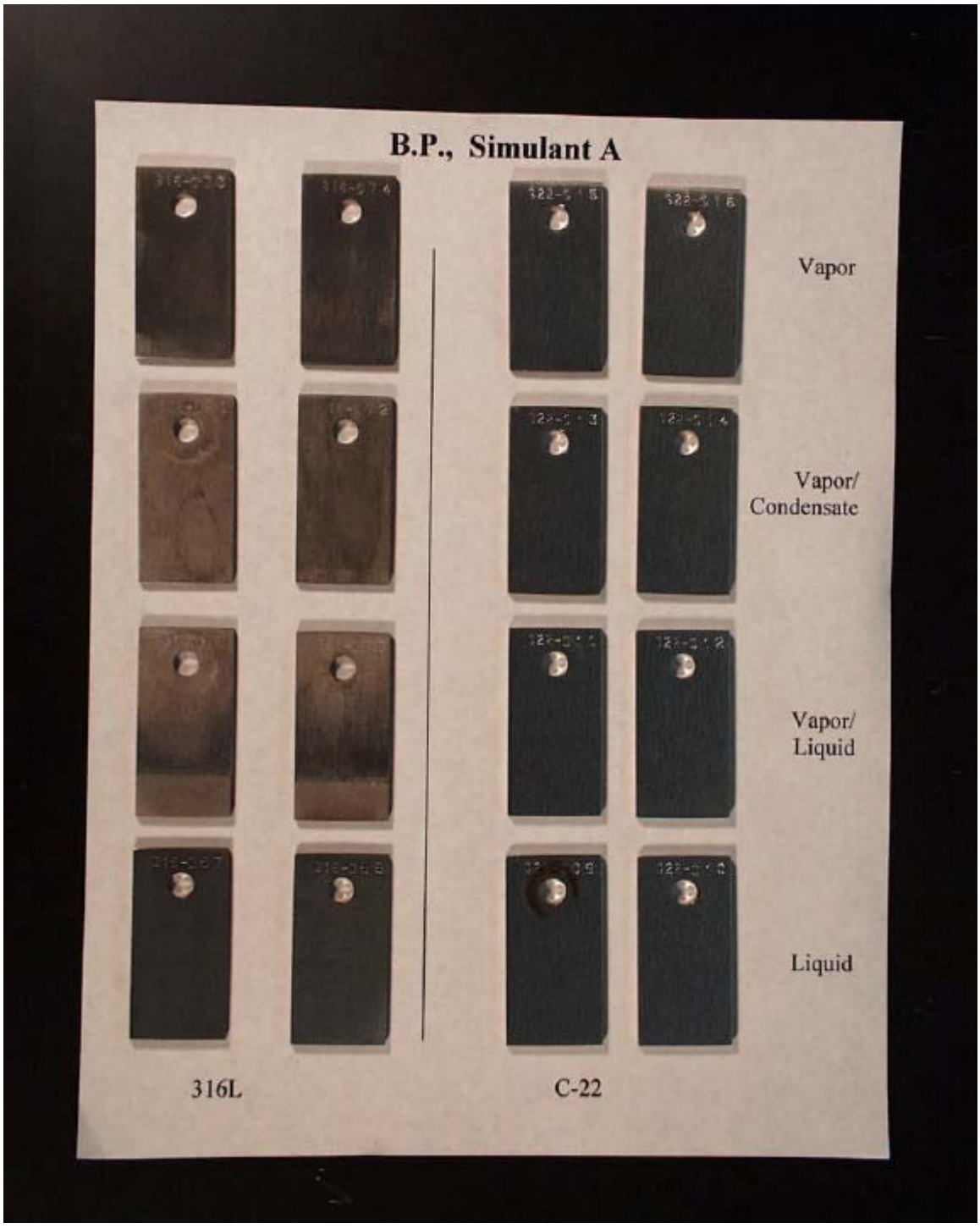

Figure A2-2. Specimens exposed to Simulant A at boiling point, after cleaning.

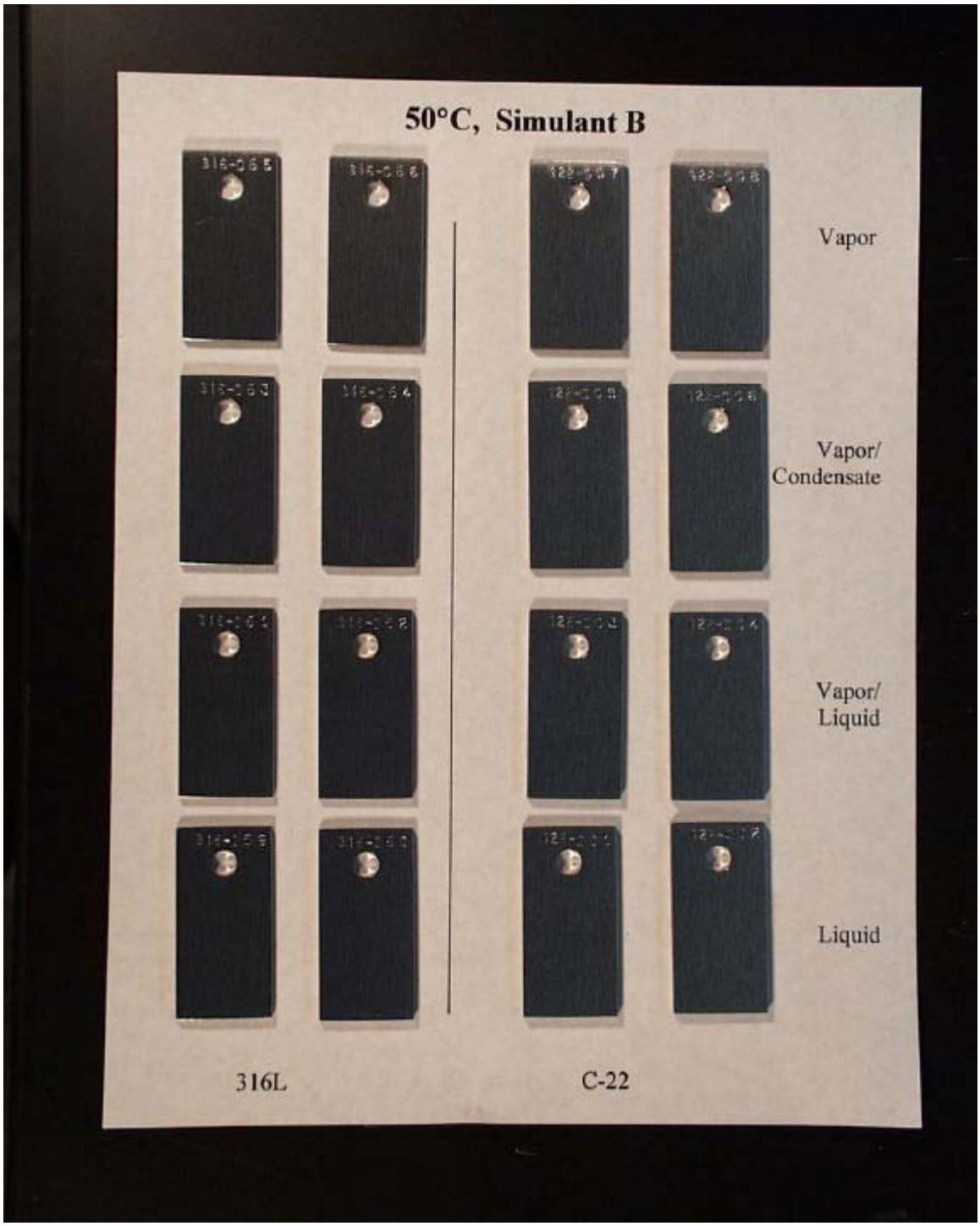

Figure A2-3. Specimens exposed to Simulant B at 50°C, after cleaning.

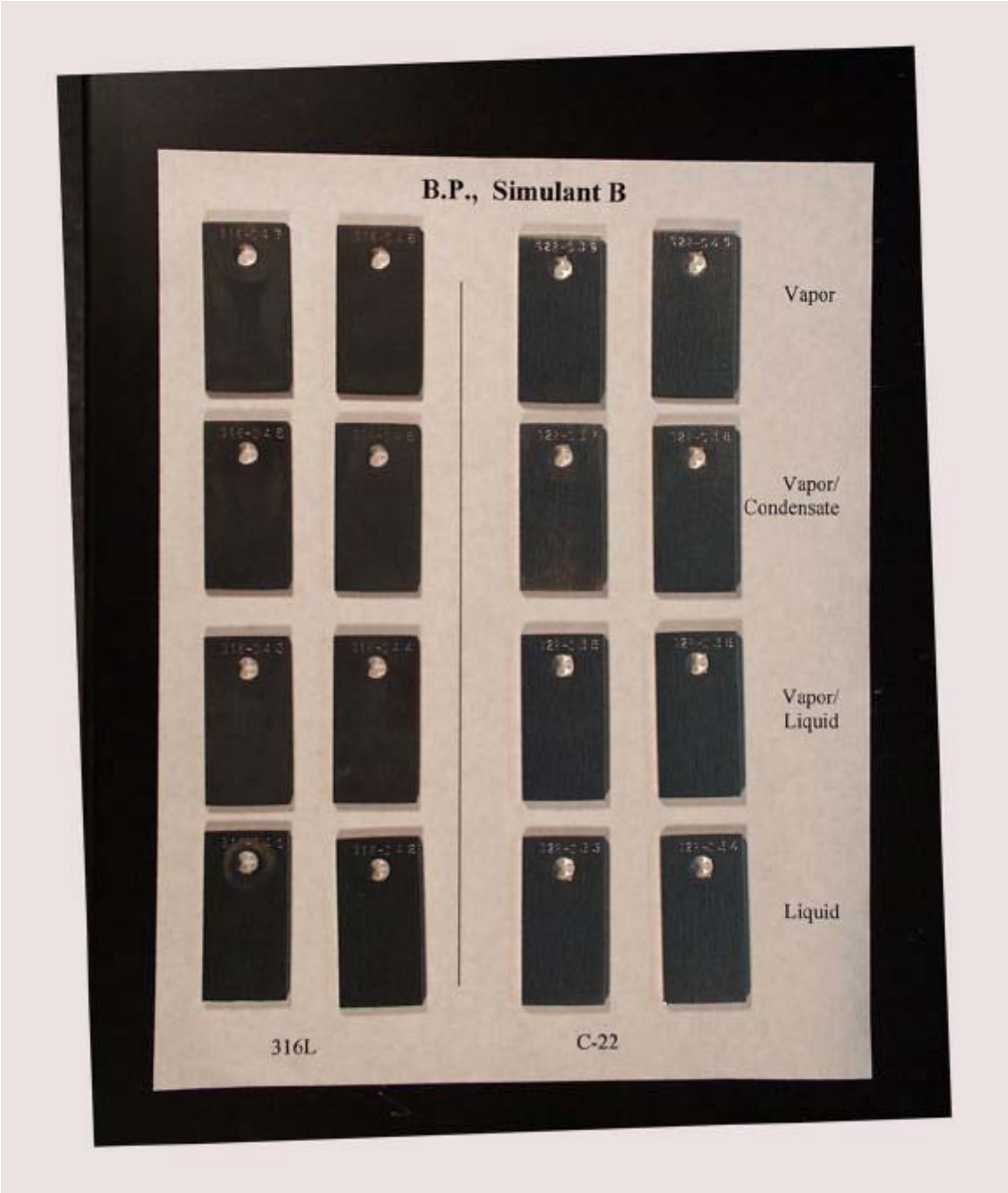

Figure A2-4. Specimens exposed to Simulant B at boiling point, after cleaning.

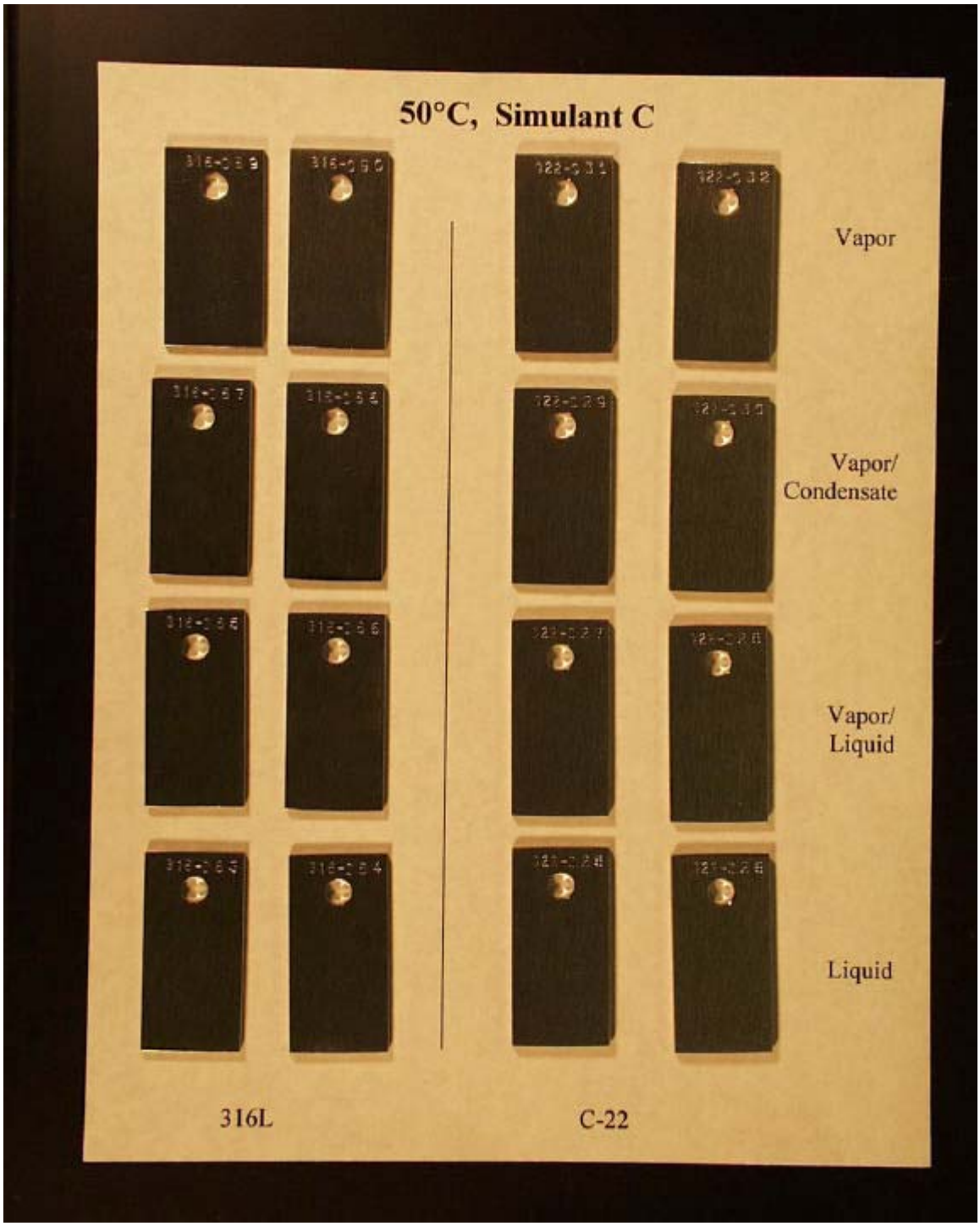

Figure A2-5. Specimens exposed to Simulant C at 50°C, after cleaning.

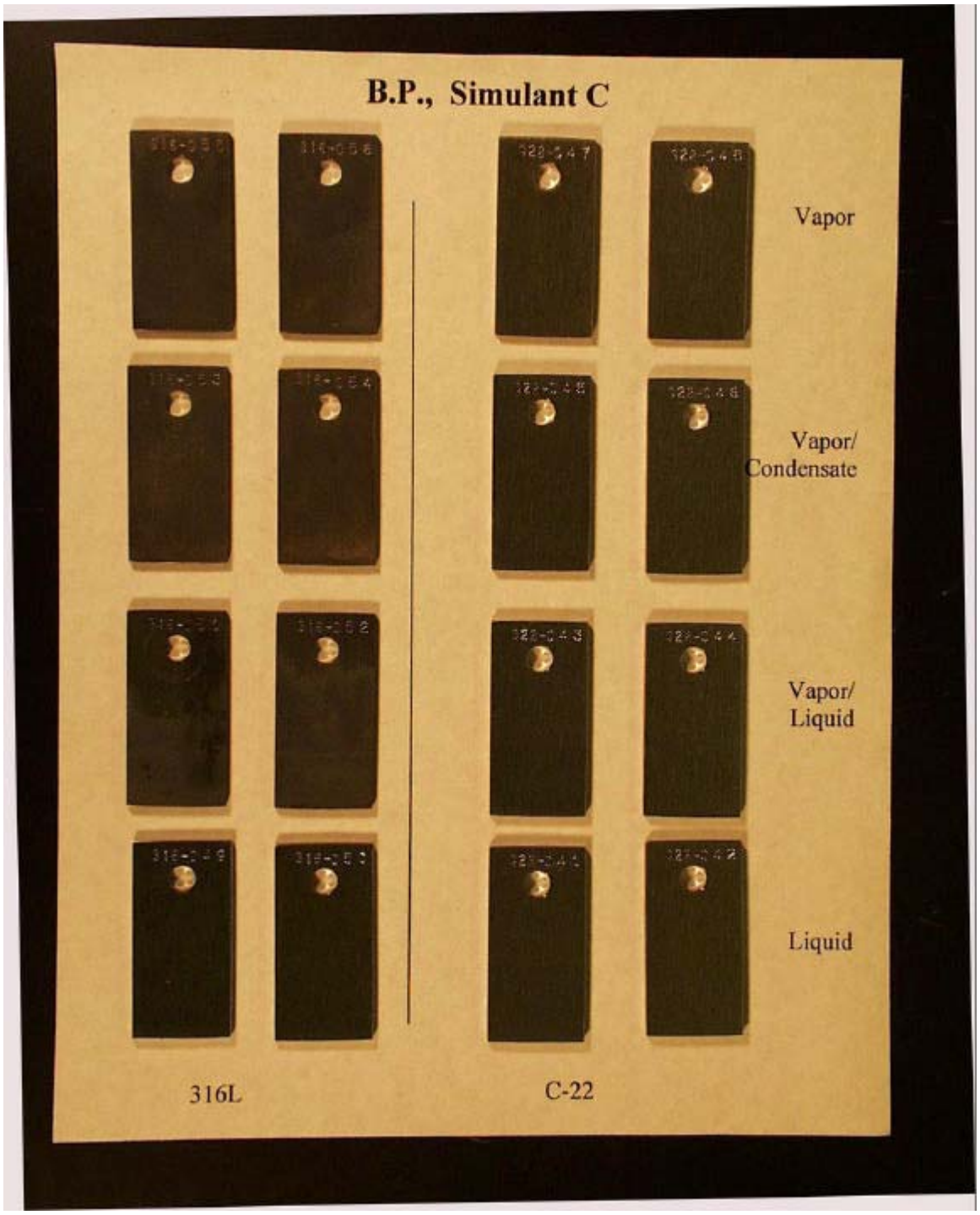

Figure A2-6. Specimens exposed to Simulant C at boiling point, after cleaning.

Appendix 3. Electrochemical Data

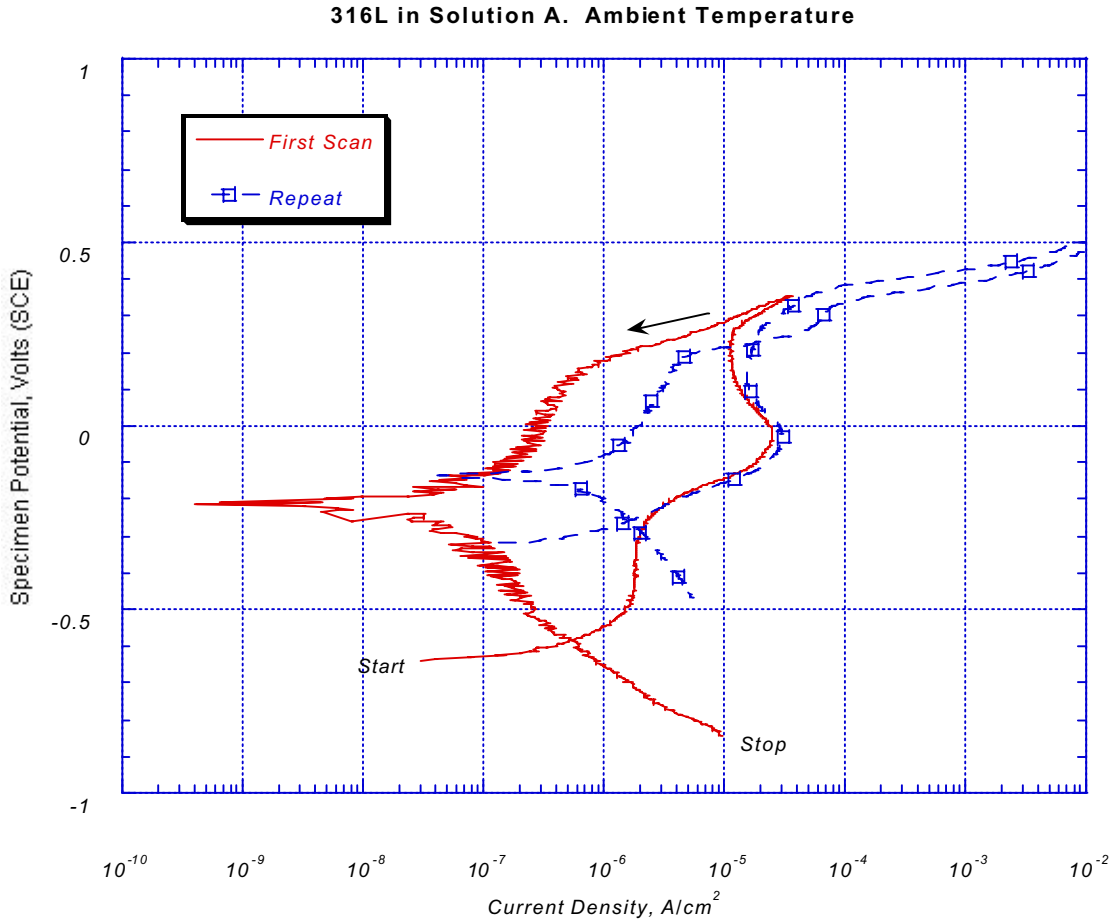

Figure A3-1. Potentiodynamic data for 316L in Solution A, ambient temperature.

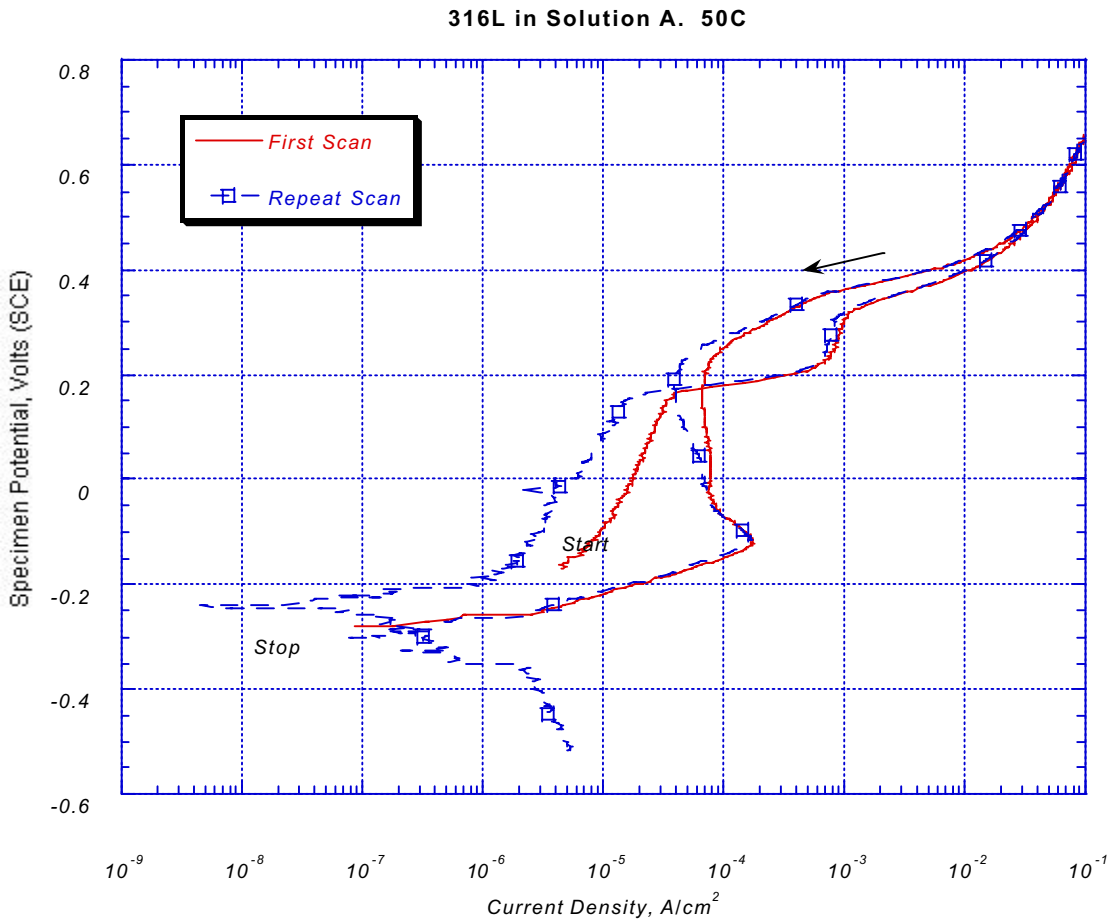

Figure A3-2. Potentiodynamic data for 316L in Solution A, 50°C.

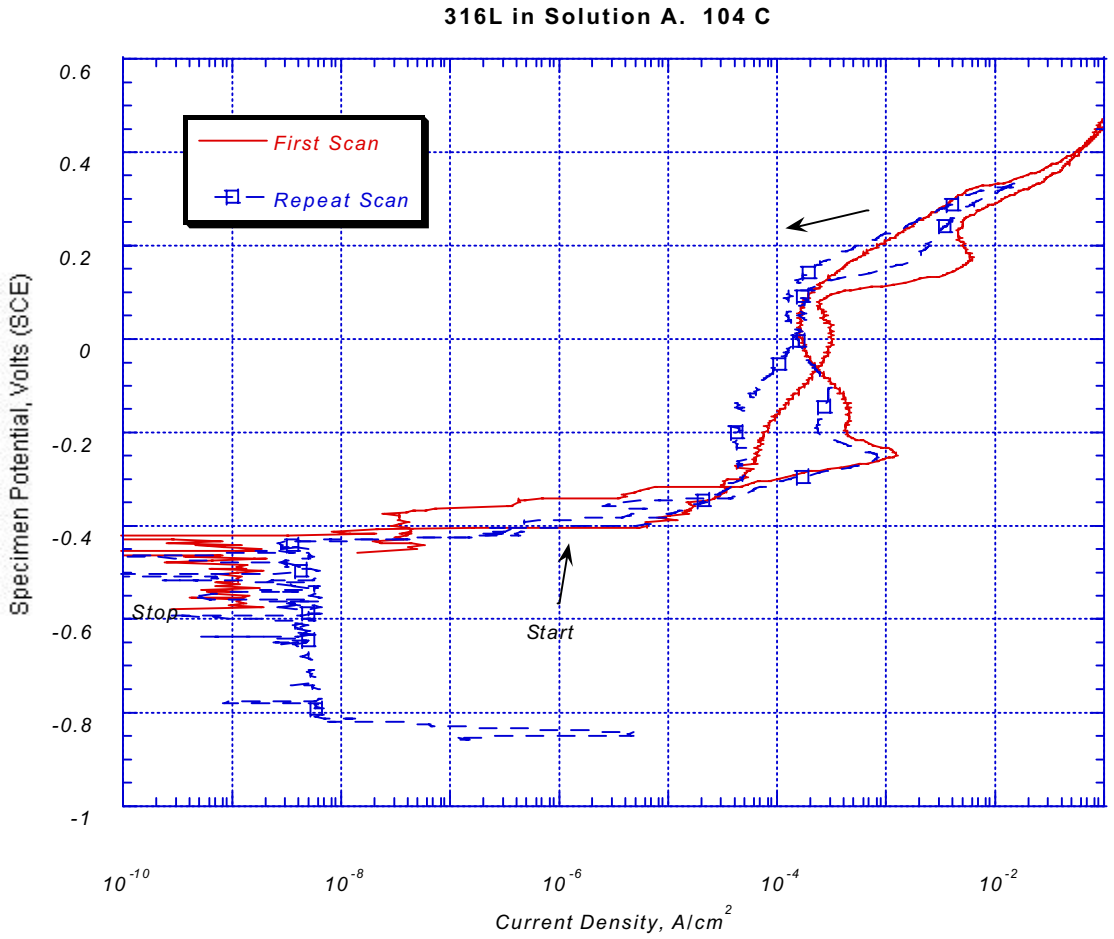

Figure A3-3. Potentiodynamic data for 316L in Solution A, 104°C.

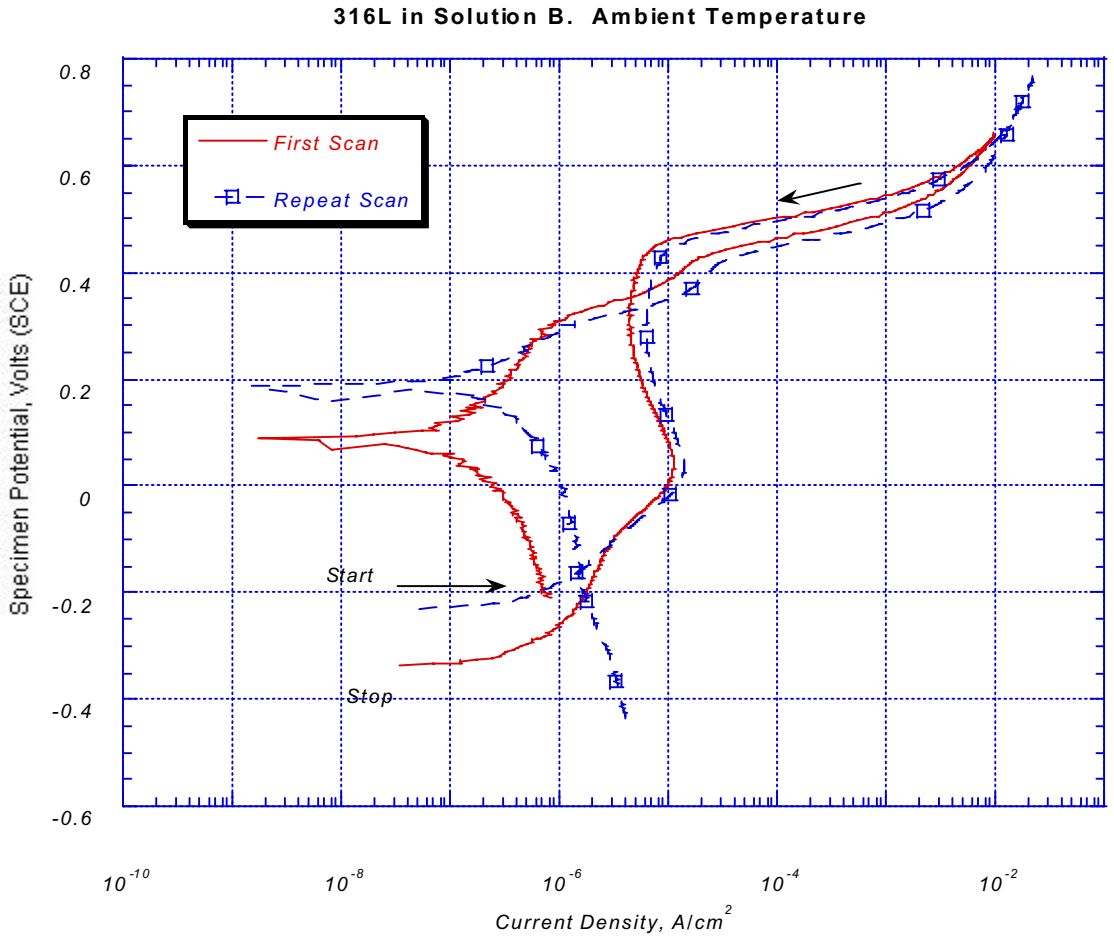

Figure A3-4. Potentiodynamic data for 316L in Solution B, ambient temperature.

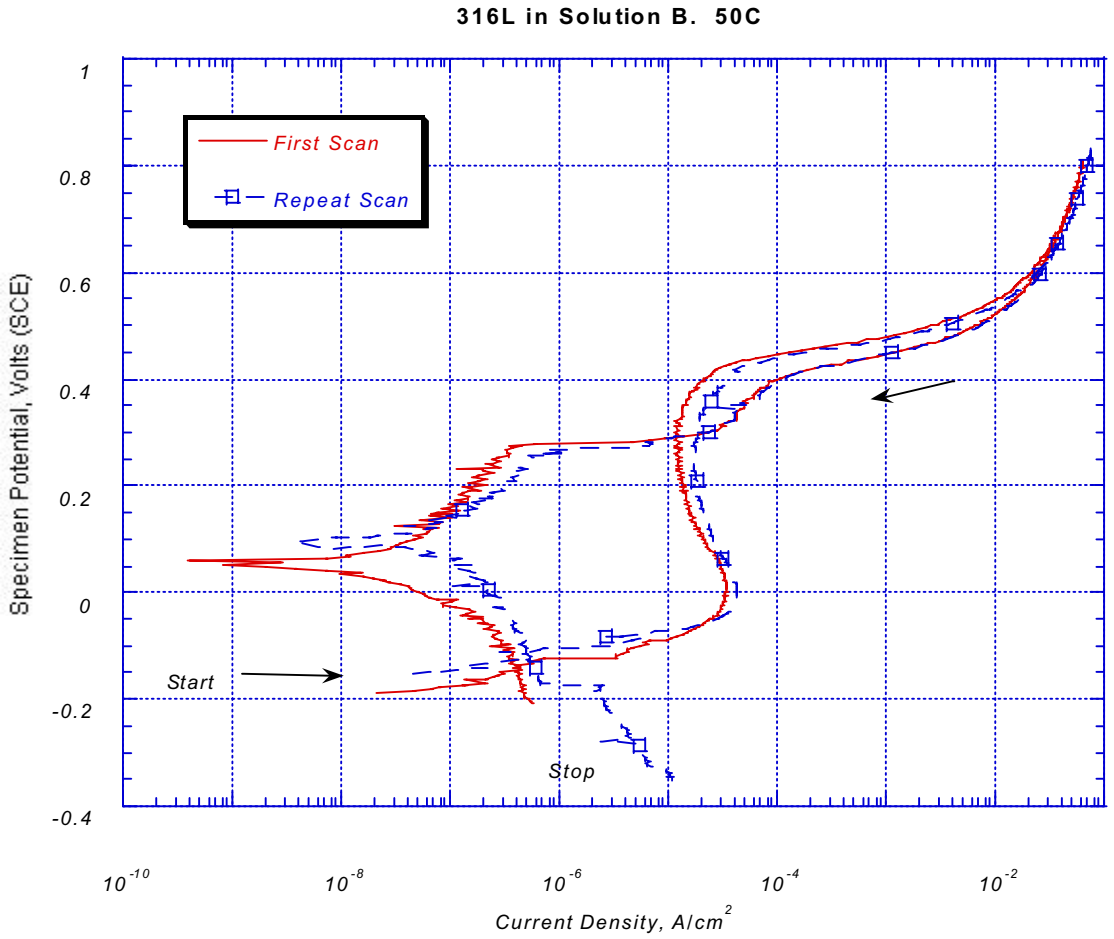

Figure A3-5. Potentiodynamic data for 316L in Solution B, 50°C.

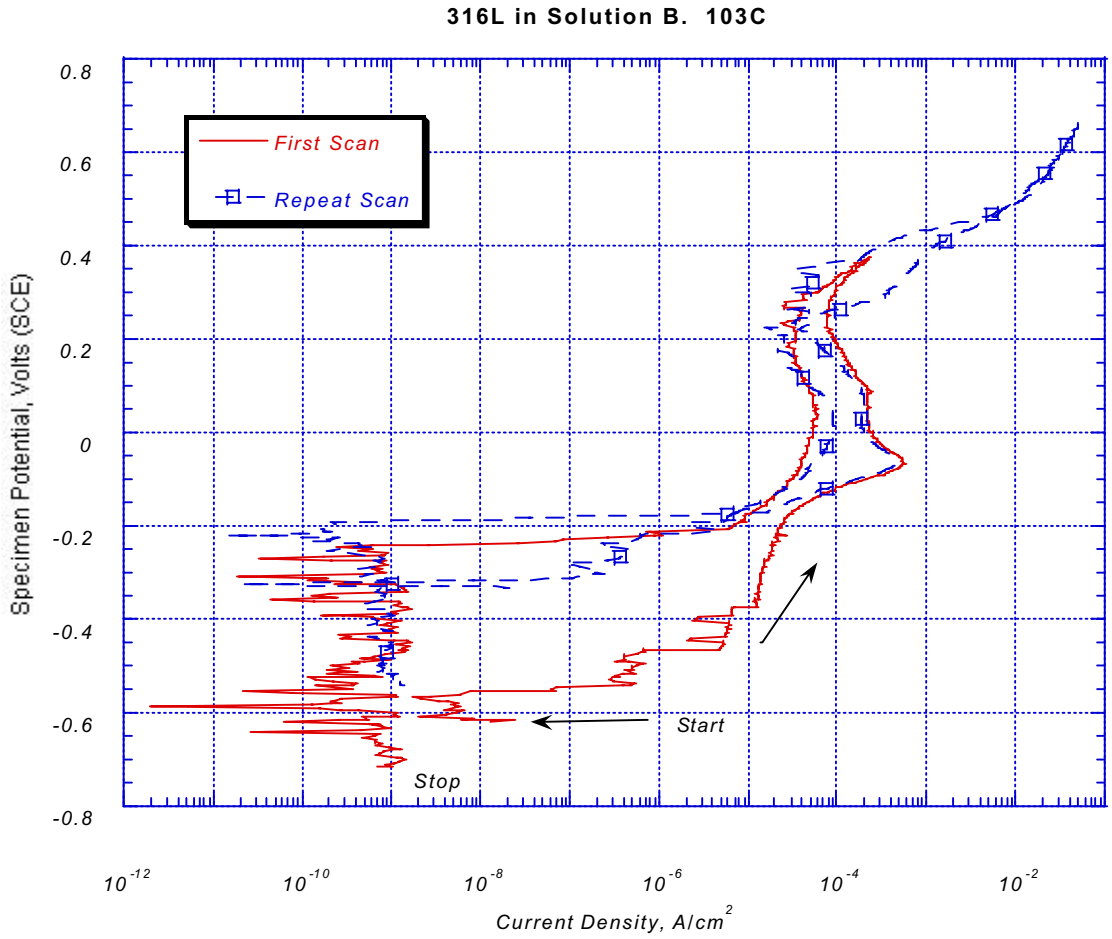

Figure A3-6. Potentiodynamic data for 316L in Solution B, 103°C.

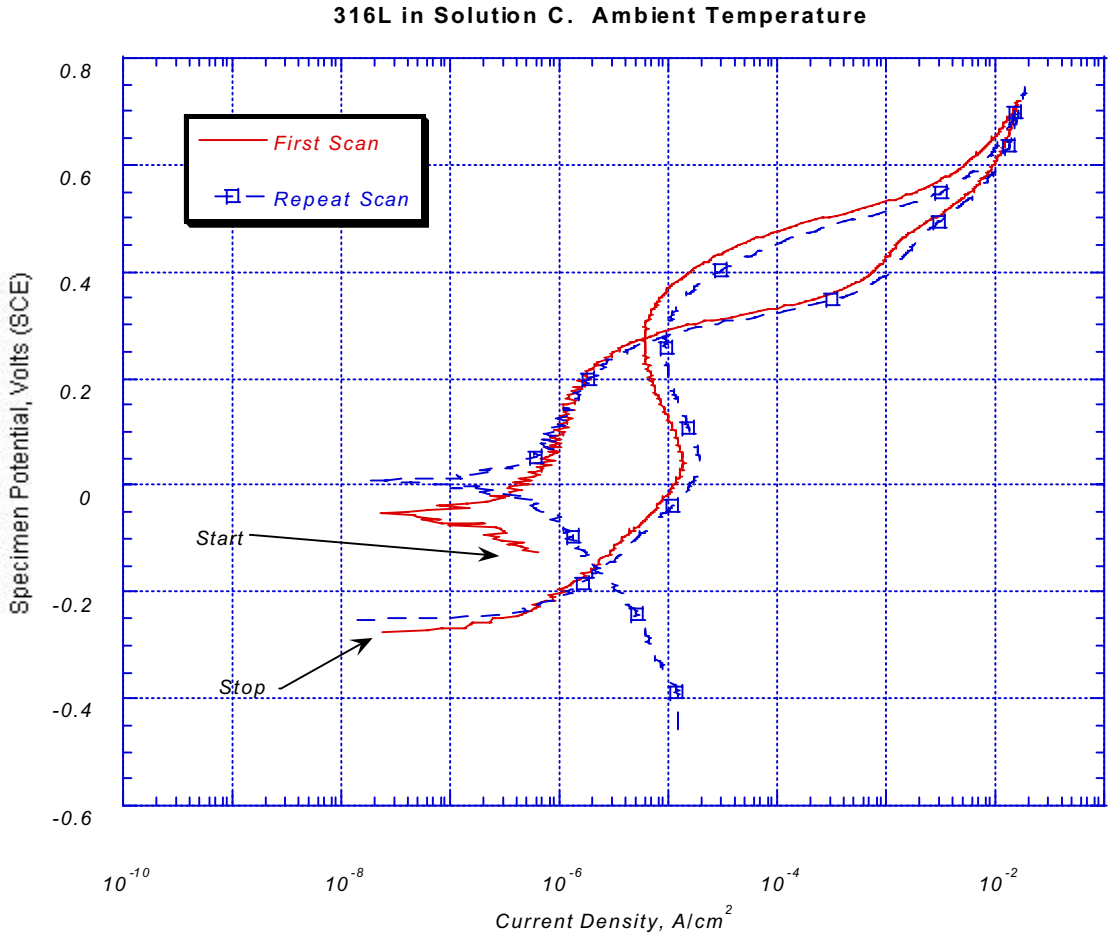

Figure A3-7. Potentiodynamic data for 316L in Solution C, ambient temperature.

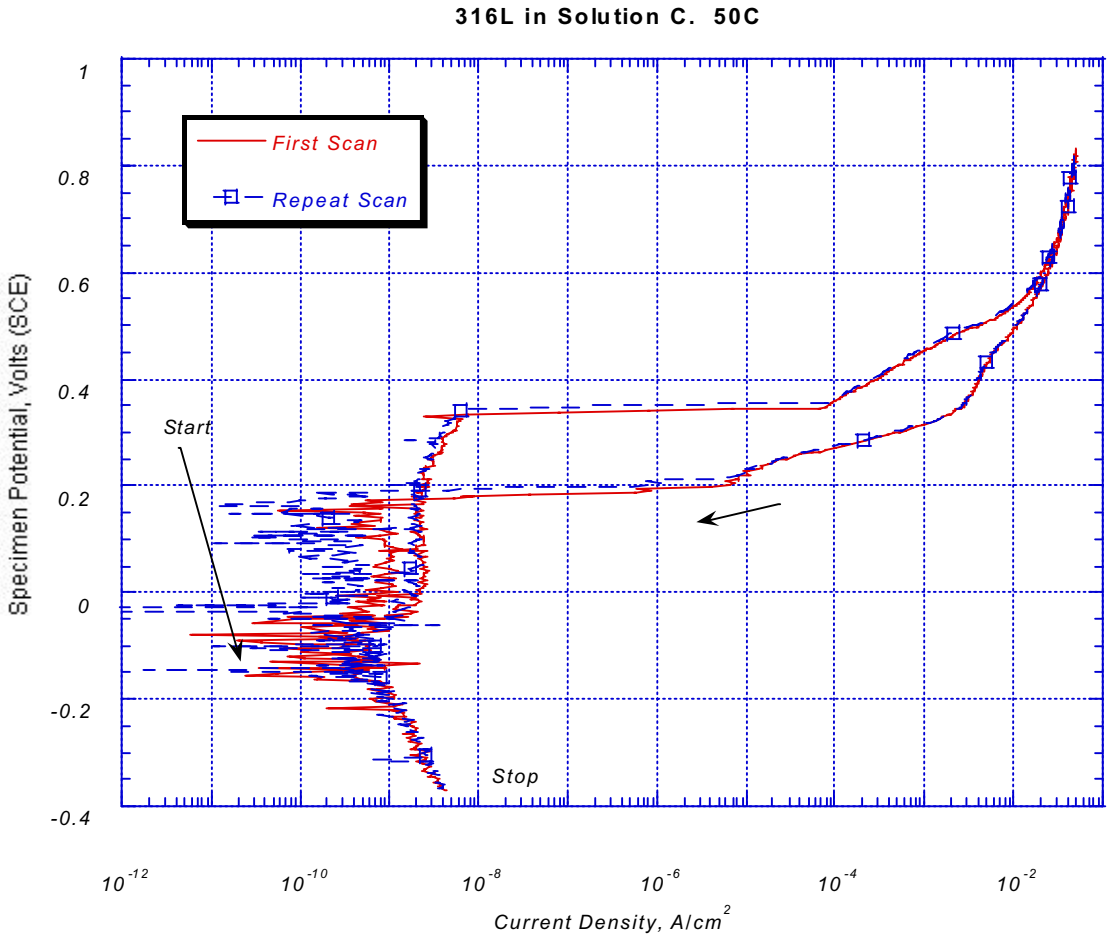

Figure A3-8. Potentiodynamic data for 316L in Solution C, 50°C.

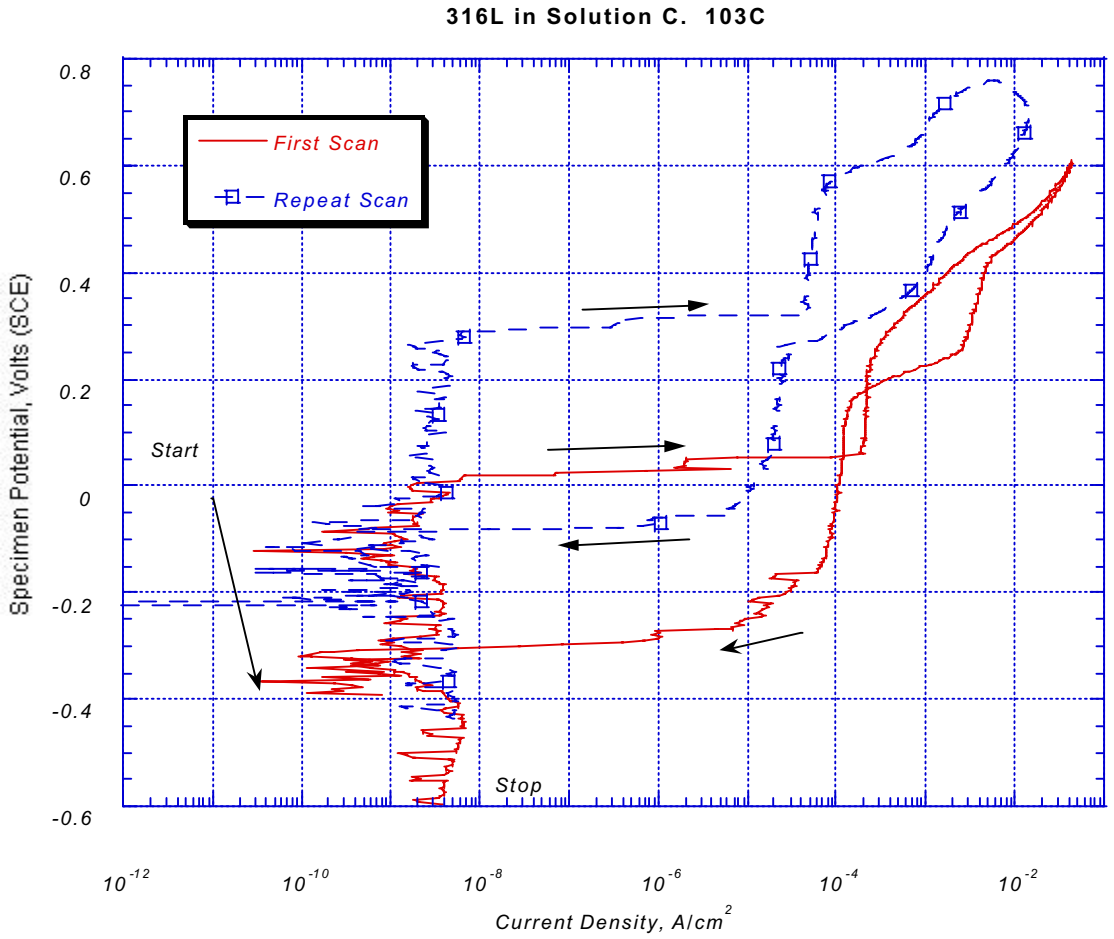

Figure A3-9. Potentiodynamic data for 316L in Solution C, 103°C.

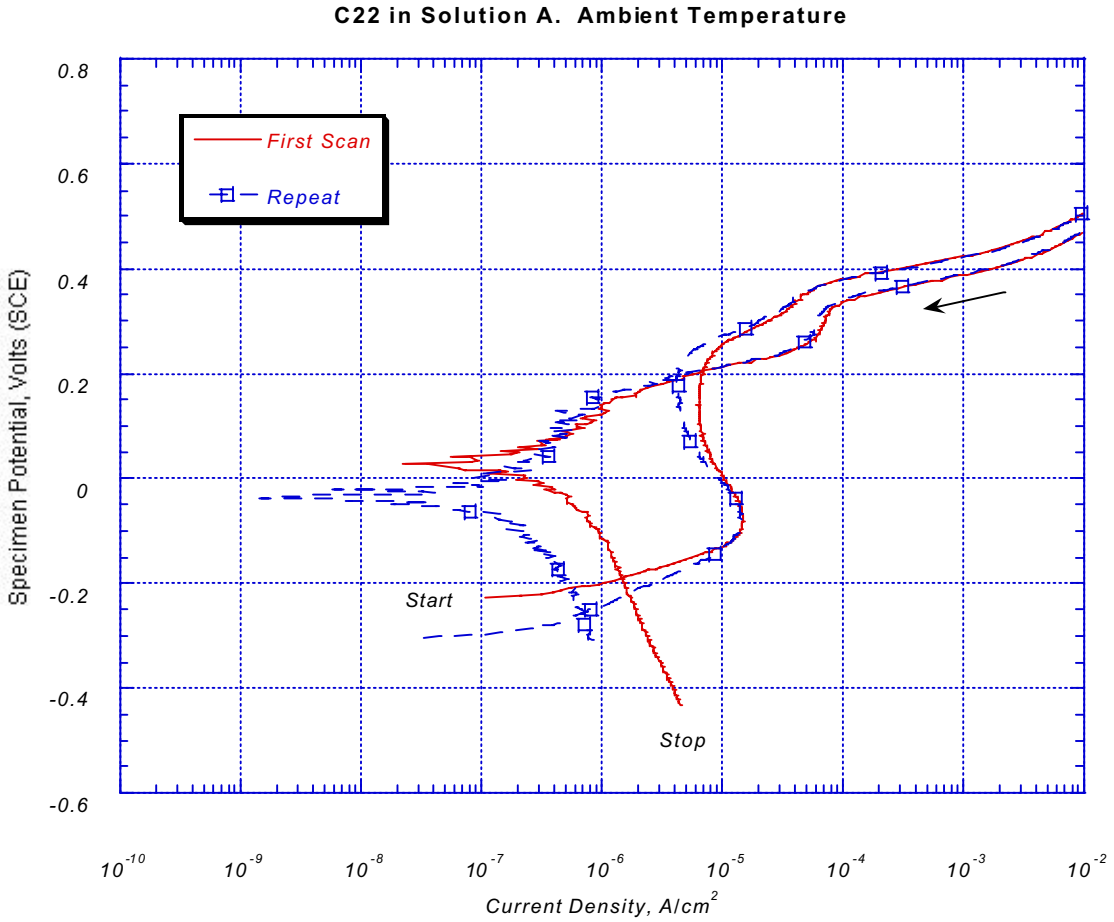

Figure A3-10. Potentiodynamic data for C-22 in Solution A, ambient temperature.

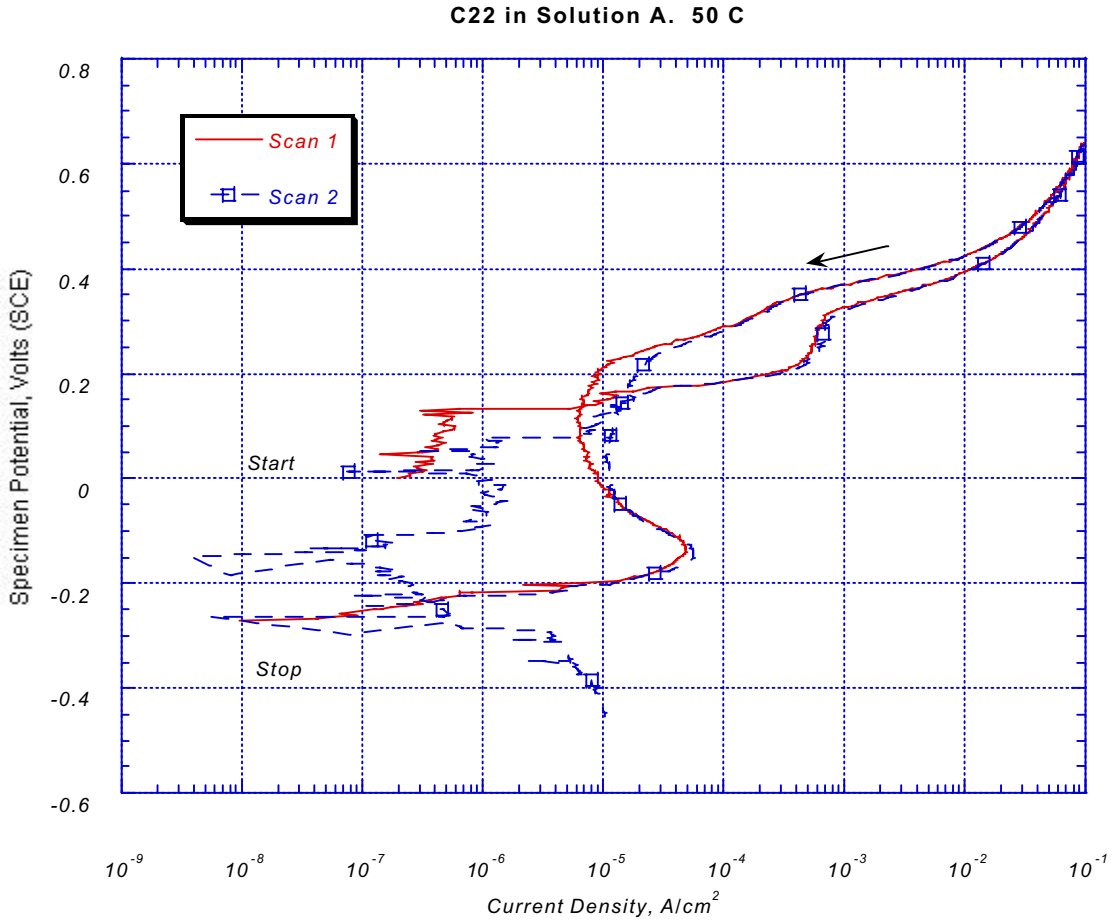

Figure A3-11. Potentiodynamic data for C-22 in Solution A, 50°C.

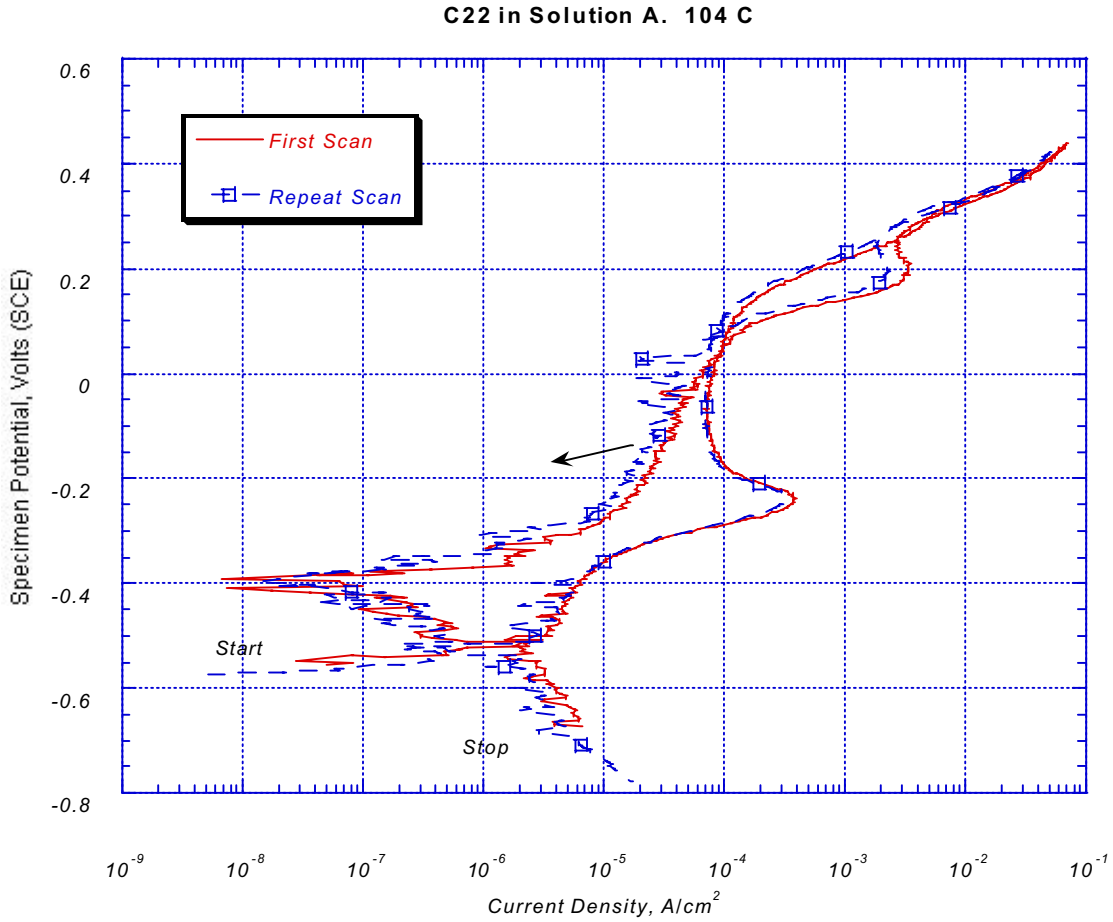

Figure A3-12. Potentiodynamic data for C-22 in Solution A, 104°C.

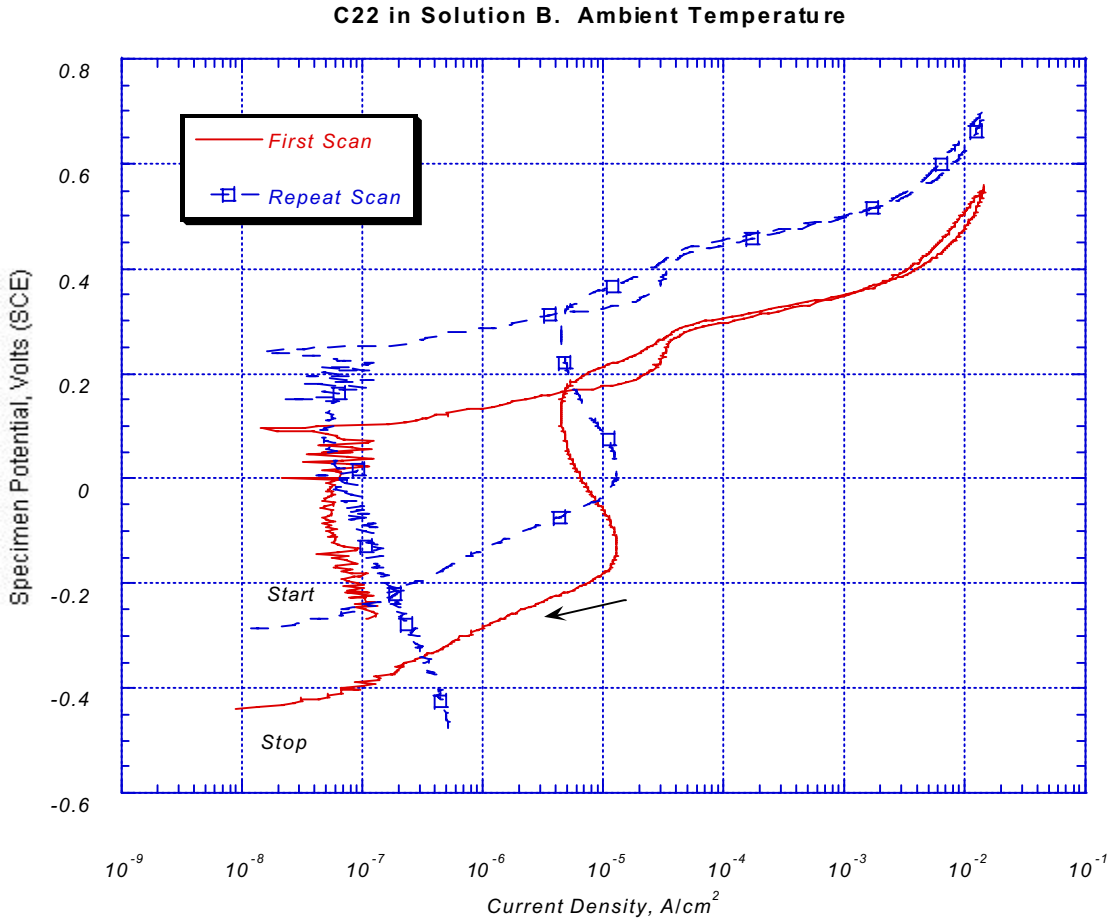

Figure A3-13. Potentiodynamic data for C-22 in Solution B, ambient temperature.

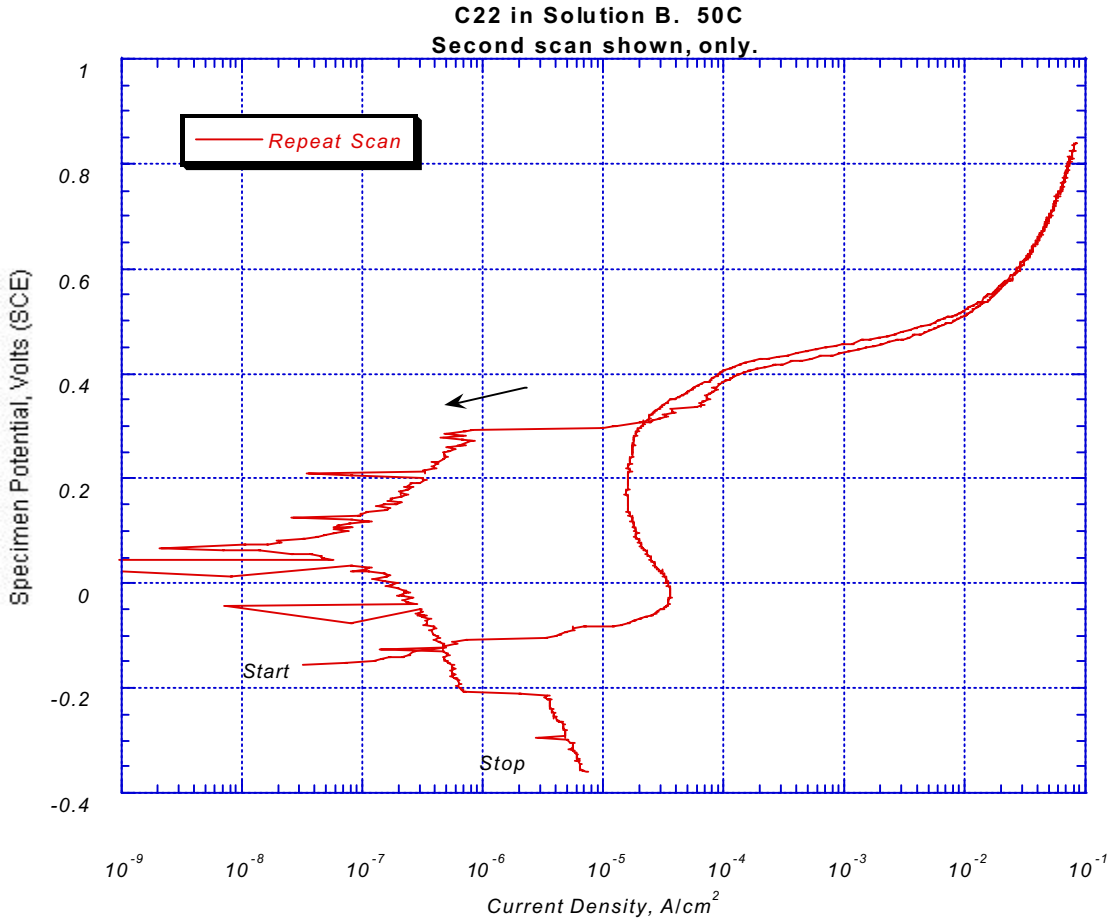

Figure A3-14. Potentiodynamic data for C-22 in Solution B, 50°C.

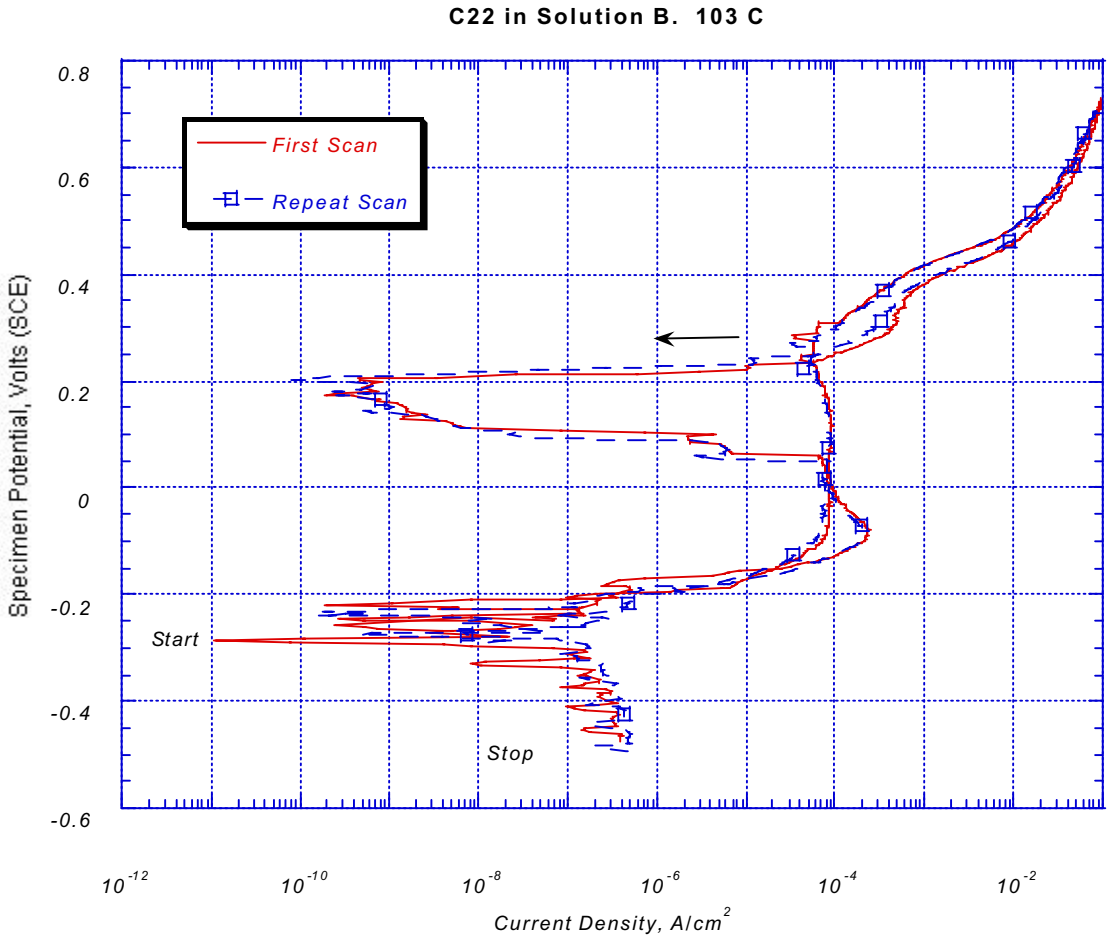

Figure A3-15. Potentiodynamic data for C-22 in Solution B, 103°C.

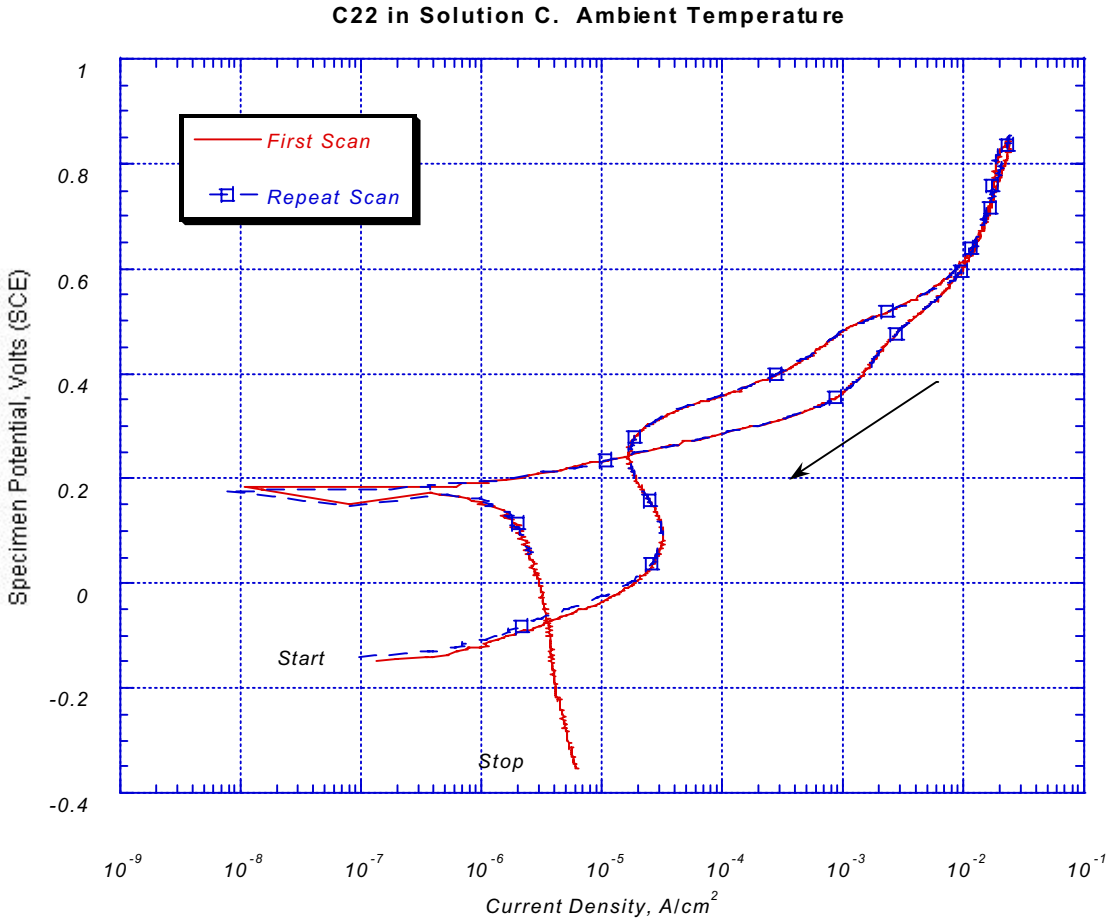

Figure A3-16. Potentiodynamic data for C-22 in Solution C, ambient temperature.

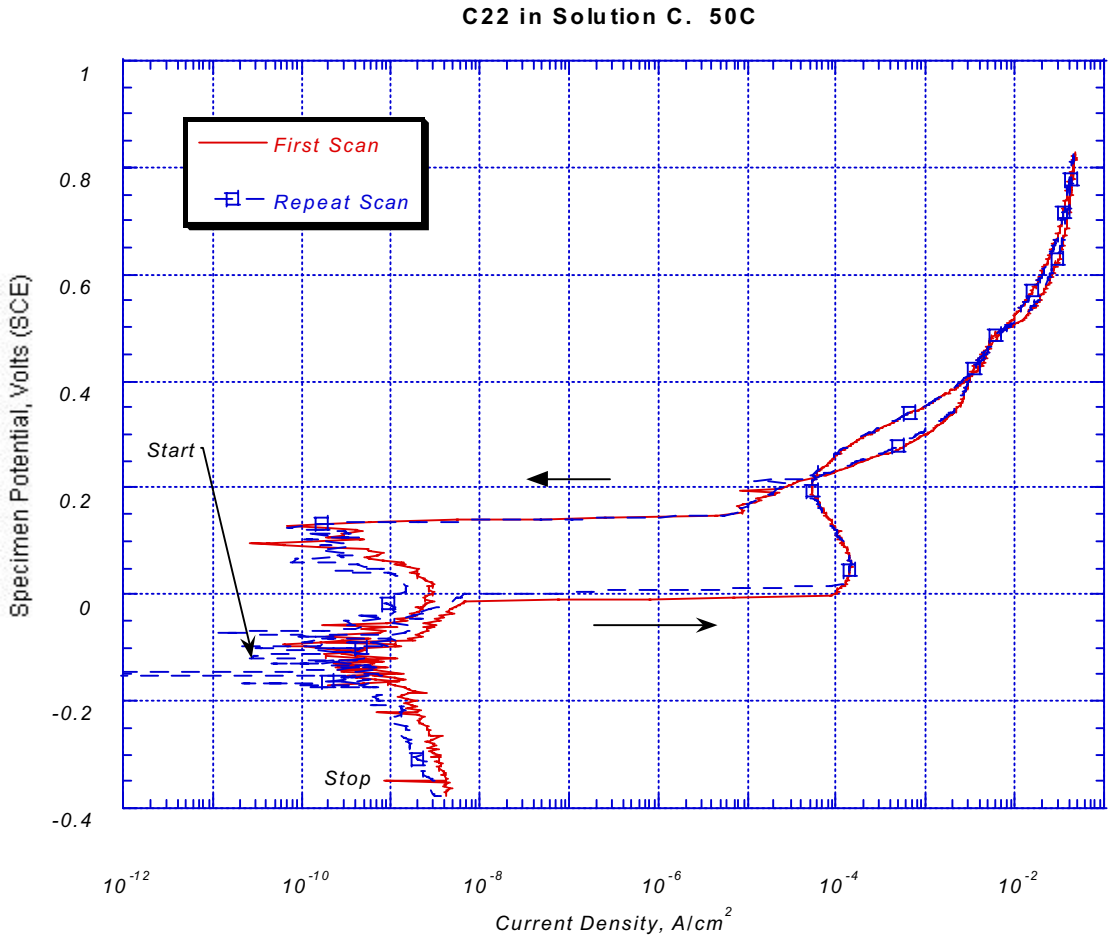

Figure A3-17. Potentiodynamic data for C-22 in Solution C, 50°C.

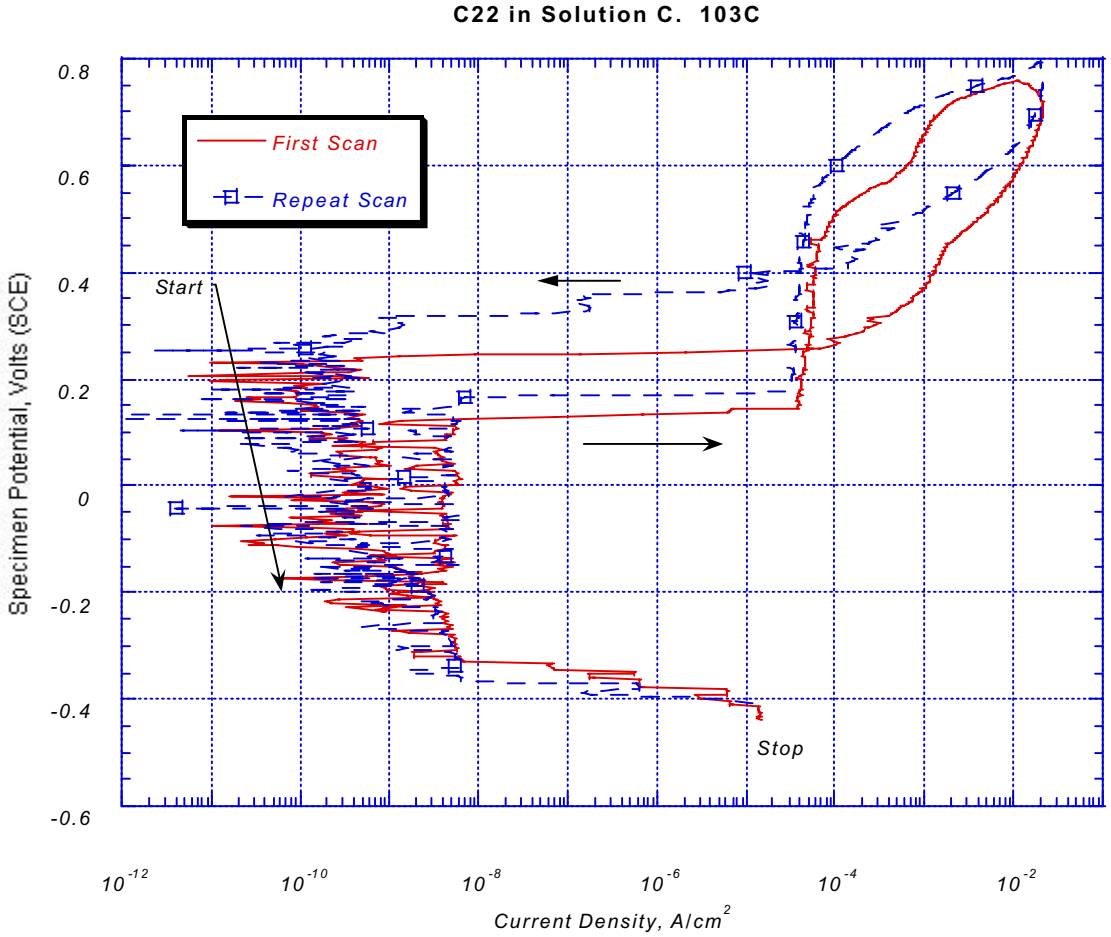

Figure A3-18. Potentiodynamic data for C-22 in Solution C, 103°C.